Models for magnetohydrodynamics of aluminium electrolysis cells

V. Bojarevics

University of Greenwich, Park Row, London SE10 9LS, UK

Abstract
The electric current and the associated magnetic field in aluminium electrolysis cells create effects limiting the cell productivity and possibly cause instabilities: surface waving, 'anode effects', erosion of pot lining, feed material sedimentation, etc. The instructive analysis is presented via a step by step inclusion of different physical coupling factors affecting the magnetic field, electric current, velocity and wave development in the electrolysis cells. The full time dependent model couples the nonlinear turbulent fluid dynamics and the extended electromagnetic field in the cell, and the whole bus bar circuit with the ferromagnetic effects. Animated examples for the high amperage cells are presented. The theory and numerical model of the electrolysis cell is extended to the cases of variable cell bottom of aluminium layer and the variable thickness of the electrolyte due to the anode non-uniform burn-out process and the presence of the anode channels. The problem of the channel importance is well known (Moreau-Evans model) for the stationary interface and the velocity field, and was validated against measurements in commercial cells, particularly with the recently published 'benchmark' test for the MHD models of aluminium cells [1]. The presence of electrolyte channels requires also to reconsider the previous magnetohydrodynamic instability theories and the dynamic wave development models. The results indicate the importance of a 'sloshing' parametrically excited MHD wave development in the aluminium production cells.

Introduction

MHD problem for aluminium electrolysis cells is of increasing importance due to significant electrical energy costs, disruptions in the technology and control of environmental pollution rate. The electric current with the associated magnetic field create effects limiting the cell productivity and possibly cause an instability of the interface between liquid aluminium and electrolyte. Moreau and Evans [2] applied the linear friction model for the horizontal circulation velocity and introduced models for the electrolyte channels surrounding the anodes, their influence on the circulation and the metal-bath interface deformation. Actually, the linear friction and the variable bottom effects are used widely in the sea wave theoretical studies [3]. The linear friction is a simplification of the more general nonlinear bottom friction term appearing in the shallow water models [4].

According to the Moreau and Evans [2] the interface deformation in the stationary case increases very significantly when the electrolyte channels are accounted. However for unstationary or stability problems in the aluminium electrolysis cells the models used are typically restricted to the mathematical developments without the inclusion of the electrolyte channels, see for example [5-8]. Recently a theory and numerical model of the 'shallow layer' electrolysis cell was extended to the cases of variable bottom of aluminium pad and the variable thickness of the electrolyte due to the anode nonuniform burn-out process and the presence of the side channels[9]. However, in the theoretical development [9] the free surface presence in the electrolyte channels was not accounted for, effectively assuming that the rigid lid surface condition is imposed for the channels and the anode bottom.

The problem of the interface calculation appeared in the light of the recent paper [1] providing a clear 'benchmark' test for the stationary interface and the velocity field in the liquid metal. During the first attempts to apply the numerical model [9] we obtained an interface shape which was quite different from that presented in [1], therefore we reconsidered the theory by including the free surface effects for the bath filled deep channels. The inclusion of the channels permits to develop a simple extension of the shallow water theory. The new version is directly applicable to the previous full nonlinear wave model and the dynamic interaction with the electromagnetic field as it is implemented in the MHD numerical code.

Mathematical model for the deformation of interface

The full description of the theory is given in the previous publications, see [9] and the references therein. Here we will repeat just the main points in the derivation and will stress the differences introduced by the free surface on the top of the channels. In the present extension of the theory for a variable layer depth we will assume that the layer deformation is small, except for the channels whose effect will be expressed as a hydrostatic 'connected vessels' principle. The shallow water model derivation starts with the assumption that the vertical momentum equation for a small depth fluid reduces to quasi-hydrostatic equilibrium between the vertical pressure p and the gravity g:

$$p(x,y,z) - p(H\ ) = -\rho g(z-H), \tag{1}$$

where the reference height *H(x,y,t)* can be chosen as the common surface for both liquid layers – the unknown interface between the metal and bath. The hydrostatic pressure distribution gradient in the horizontal direction does not depend on vertical coordinate in the respective layer, as can be seen from (1). If the top surface of the bath layer is H_t , then the pressure at the top of rigid lid enclosed channels will be obtained from the full solution. However, if there is a free surface on top of the bath channels, then $p(H_t) = 0$, and the pressure at the variable interface H is related by the hydrostatics to the local position only:

$$p(H) = \rho_2 g(H_t - H(x,y,t)), \tag{2}$$

where for clarity we added the index '2' for the bath layer properties. According to the Moreau & Evans [2], the surface H_t in the channels is practically flat and equal in all channels. If the channels (side, middle and between the individual anodes) are sufficiently deep, say 2-3 or more times the ACD, then this hydrostatic pressure will effectively act in all electrolyte layer, similarly to connected vessels principle. The electromagnetic force in the electrolyte will give very little modification to this dominant hydrostatic pressure. Then from (2) follows an approximated pressure gradient variation in the electrolyte at the variable interface *H(x,y)*:

$$\partial_x p(H\ ) = -\rho_2 g \partial_x H; \qquad \partial_y p(H\ ) = -\rho_2 g \partial_y H\ . \tag{3}$$

Having stated the approximations for the pressure and its horizontal gradient in both the shallow layers, we can state the horizontal momentum equations for the depth average non-dimensional quantities. For simplicity we will consider initially the stationary case only. The Moreau & Evans model [2] is based on the linear equations for the two fluid layers:

$$0 = -\partial_j p - \mu \hat{u}_j + \hat{f}_j; \qquad \partial_j \hat{u}_j = 0\,, \tag{4}$$

where the indexes *j* = (1 or 2) represent respectively *x, y* coordinates, the summation over repeated indexes *j* means the divergence free depth average velocity field. After substituting the depth independent pressure gradient from (3), the horizontal momentum equations are

$$0 = -\partial_j p(H) - \rho_i g \partial_j H - \mu \hat{u}_j + \hat{f}_j\ . \tag{5}$$

The common pressure *p(H)* at the interface can be eliminated by taking the difference between the equations in the two layers, characterized each by the respective index: i=1 (aluminium) and i=2 (electrolyte). The unknown interface shape will be determined by solving the resulting equations coupled to the velocity field. When the channels are absent, the friction coefficient can be assumed as a constant in each layer, and the equation (5) gives the second order equation for the interface:

$$(\rho_1 - \rho_2) g \partial_{jj} H = \partial_j (\hat{f}_{j1} - \hat{f}_{j2})\ . \tag{6}$$

The boundary conditions are derived from the zero normal velocity condition at the cell walls. However, in the presence of the bath channels the approximation of a constant friction is not valid, dropping to a very low value in the channels. Therefore the divergence operator applied to (5) will not eliminate the velocity field from the interface equation. The coupling to the intense velocity near the channels can be eliminated, to a certain approximation discussed previously, if applying the hydrostatic pressure gradient (3) directly in the equation (5) stated for the aluminium (*i* = 1) layer only:

$$0 = -(\rho_1 - \rho_2) g \partial_j H - \mu_1 \hat{u}_{1j} + \hat{f}_{1j}\,. \tag{7}$$

The continuity of the pressure at the interface is satisfied by choosing the pressure *p(H)* at the common interface. The bottom friction in the aluminium is constant according to the Moreau & Evans model, and the divergence of (7) gives the stationary interface equation for the conditions with free surface deep electrolyte channels :

$$(\rho_1 - \rho_2) g \partial_{jj} H = \partial_j (\hat{f}_{j1})\ . \tag{8}$$

The horizontal circulation velocities, driven by the rotational part of the electromagnetic force, can be calculated by solving the momentum equations in the two layers. Additionally, the 2-equation turbulence model can be applied for the horizontal turbulent momentum diffusion (the effective viscosity) in more general approach. We will not consider here this part of the theory, instead focusing on the interface evolution equation modification.

Taking into account the hydrostatic pressure distribution in the presence of the channels for the full time dependent interface equation stated previously [9], we have the non-linear wave equation for the aluminium-electrolyte interface *H(x,y,t)* with the variable bottom $H_b(x,y)$ and top $H_t(x,y)$:

$$\left(\frac{\rho_1}{H-H_b} + \frac{\rho_2}{H_t - H}\right)\partial_{tt} H + \left(\frac{\rho_1 \mu_1}{H-H_b} + \frac{\rho_2 \mu_2}{H_t - H}\right)\partial_t H - (\rho_1 - \rho_2) g \partial_{jj} H = \partial_j(-\hat{f}_{j1}) - \tfrac{1}{2}(H - H_b)\partial_{jj} \hat{f}_{z1} - [\rho_1 \partial_j(\hat{u}_{k1}\partial_k \hat{u}_{j1}) - \rho_2 \partial_j(\hat{u}_{k2}\partial_k \hat{u}_{j2})] \tag{9}$$

The linear stability models can be recovered from (9) by excluding the nonlinear horizontal velocity term (containing

the rotational and potential parts), the vertical electromagnetic force component f_z contribution, and assuming the H_b and H_t as constants. The nonlinear equation (9) extends the wave description to the weakly nonlinear and slowly varying top and bottom cases in the presence of electrolyte channels. The complexity of any practically usable MHD model arises from the coupling of the various physical effects: fluid dynamics, electric current distribution, magnetic field and thermal field. Magnetic field in an aluminium cell is created by the currents in the cell itself and from the complex bus-bar arrangement around the cell, in the neighboring cells and the return line, and by the effect of cell construction steel magnetization. The general MHD model, presented previously [9], accounts for the time dependent coupling of the current and magnetic fields with the bath-metal interface movement. The magnetic field from the currents in the full bus-bar network is recalculated at each time step during the dynamic simulation using the Biot-Savart law.

Results for 180 kA cell

The numerical solution of the described MHD model uses a mesh of 128x64x2 and a spectral function representation in the space of each fluid layer. This ensures a good accuracy solution and enables one to re-compute the electromagnetic and fluid dynamic field time dependent distribution in a reasonable computational time if required. The paper [1] provides several 'benchmark' tests for the aluminium electrolysis cell MHD models regarding the stationary fields only. The second test requires to compute the electric current in both fluid layers from the given distribution at the top (uniform from all anodes) and the bottom as

$$j_z = -5625 - 2500\,y^2 \quad (\mathrm{A/m^2}) \ , \tag{10}$$

where the coordinate origin is the middle of the flat bottom of the cell. The electric current computed by the MHD code for these conditions is represented in the Figures 2 and 3. The presence of the channels is clearly seen for the electrolyte layer in the Figure 2. The magnetic field is assumed to be given in both fluid layers independent of the vertical coordinate z:

$$B_x = 6y \cdot 10^{-3}, \quad B_y = (-3x + 1.5) \cdot 10^{-3}, \ B_z = (xy + 0.5) \cdot 10^{-3}, \ (\mathrm{T}) \tag{11}$$

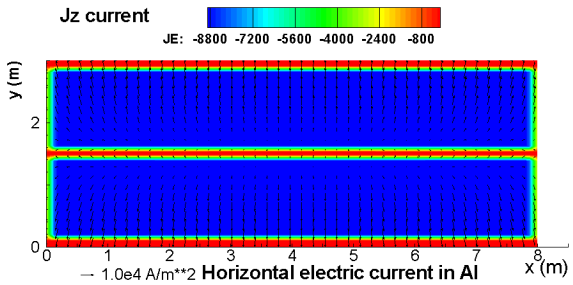

Fig. 1: The computed electric current in the liquid metal with the prescribed bottom distribution

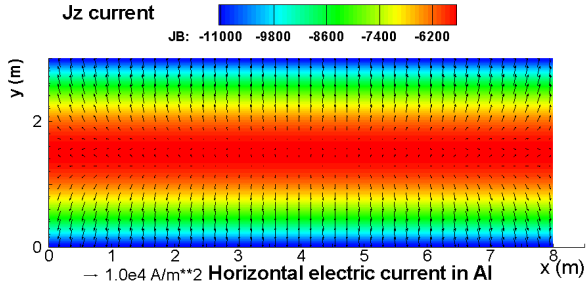

Fig. 2: The computed electric current in the electrolyte with the channels.

The electromagnetic force distribution is computed for the given magnetic field and the electric current (shown in Figures 1 and 2), then there are no electromagnetic force in the electrolyte channels, but the overall force distribution and magnitude are quite similar in both layers. Therefore it is not surprising to find the interface deformation being very small and slightly inflected in the middle (because of the larger electrolyte force concentration there) as shown in the Figure 3 for the case without the effect of the electrolyte channel free surface. There is practically a balance between the 'pinching' effects of the forces in the two layers. A strikingly different interface deformation (Figure 4) is obtained when using the model equation (8), or even (9), with the hydrostatic pressure dominating in the electrolyte. For the comparison with the published 'benchmark' results [1] the Figure 4 shows a very close correspondence.

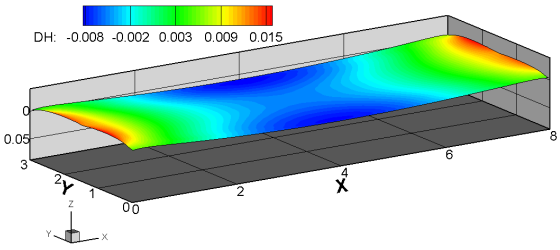

Fig. 3: The computed metal-bath shape without the open channel effect.

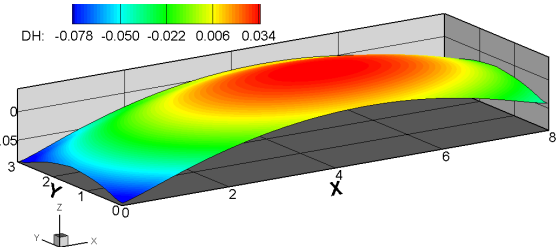

Fig. 4: The computed metal-bath shape with the open channel effect.

The accurate representation of the interface depends on a number of additional conditions, like for instance, the anode bottom being burnt out to the profile corresponding to the actual interface and corresponding electric current redistribution for the constant ACD. For further tests the velocity fields were computed. The computed velocity in the electrolyte, as computed with the presented MHD code, is very similar qualitatively to that predicted by Moreau & Evans [2], clearly showing the effects of the intense recirculation in the channels. The flow is sufficiently intense and develops significant turbulence, which leads to a redistribution of the velocity field. The established velocity field for the aluminium layer is very similar to that predicted in [1] as a part of the 'benchmark' tests.

Since we have derived a new modification of the time dependent interface model, given by the equation (8), or (9), we need to investigate the consequences of the free surface channels on the possibly unstable behavior of the electrolysis cell. For this purpose a model bus network for a 180 kA cell was set up. This permits to run the full MHD time dependent code including the coupling of the fields. The horizontal electric currents in the liquid affect the magnetic field, making it 3-dimensional and different at the top and bottom of the metal layer. For this model cell the initial deformation of the liquid metal surface (usually assumed to be a 'stationary' interface), as computed with the effect of the free electrolyte channels. The distribution of the magnetic field in this cell leads to an unstable wave development, as illustrated in the Figure 7. The time history shows also the instructive comparison with the wave development in case without the presence of the free electrolyte channels. Without the inclusion of the electrolyte channels with free surface the instability sets in more easily, and the time when the wave crest reaches the anode bottom is shorter. The instability type in the case without the channels is the classical rotating wave (see Figure 6) , as described in the theoretical papers [5-7]. The presence of the electrolyte channels changes the instability type, which resembles a 'sloshing' wave concentrated along the middle longitudinal line of the cell (Figure 5). The Fourier power spectra clearly demonstrate the difference in the wave frequencies: a single peak for the case with the channels, and two dominant wave frequencies for the case not accounting for the channels.

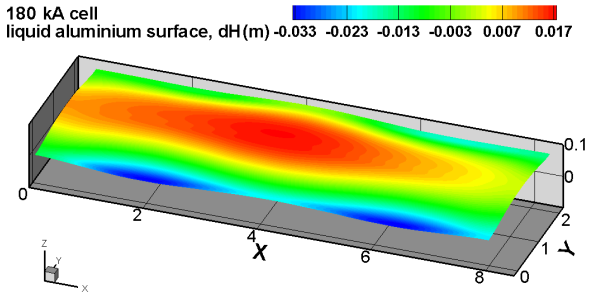

Fig. 5: Interface with steel effect and with channels.

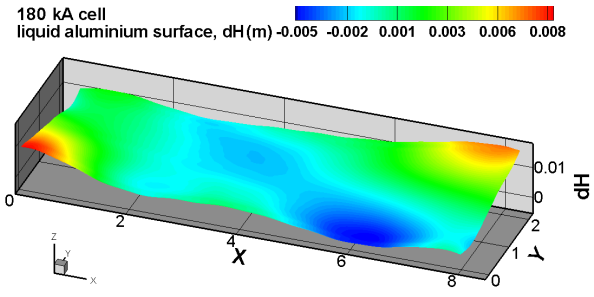

Fig. 6: Interface with steel effect and no channels.

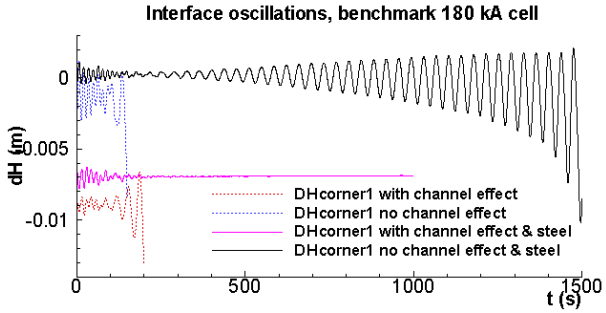

Fig. 7: Different type of instability when the channels and steel are accounted.

References

[1] D.S. Severo, V. Gusberti, A.F. Schneider, E.C. Pinto, V. Potocnik (2008), Proc. TMS Light Metals, 413-418

[2] R. Moreau, J.W. Ewans (1984), Journal of Electrochemical Society, 131, 10, 2251-2259

[3] C. C. Mei (1989), The Applied Dynamics of Ocean Surface Waves, World Scientific

[4] A.K. Rastogi and W. Rodi (1978), J. Hydraulics Division ASCE, HY3, 397-420

[5] N. Urata, K. Mori, H. Ikeuchi (1976), Keikinzoku, 26, 11, 573-600

[6] A. D. Sneyd, A. Wang (1994), J. Fluid Mech., 263, 343-359

[7] V. Bojarevics, M. V. Romerio (1994), Eur. J. Mech., B/Fluids, 13, 1, 33-56

[8] H. Sun, O. Zikanov, B. A. Finlayson, D. P. Ziegler (2005), Proc. Light Metals, TMS, 437-441

[9] V. Bojarevics, K. Pericleous (2008), Proc. TMS Light Metals, TMS, 403-408